HHS Public Access

Author manuscript

J Pathol. Author manuscript; available in PMC 2018 May 15.

Published in final edited form as:

J Pathol. 2017 December ; 243(4): 431–441. doi:10.1002/path.4983.

Hepatic inflammation caused by dysregulated bile acid synthesis is reversible by butyrate supplementation

Lili Sheng[1,†], **Prasant Kumar Jena**[1,†], **Ying Hu**[1], **Hui-Xin Liu**[1], **Nidhi Nagar**[1,2], **Karen M Kalanetra**[3], **Samuel William French**[4], **Samuel Wheeler French**[5], **David A Mills**[3], and **Yu-Jui Yvonne Wan**[1,*,iD]

[1]Department of Medical Pathology and Laboratory Medicine, University of California, Davis, Sacramento, CA, USA

[2]Department of Biological Sciences, California State University, East Bay, Hayward, CA, USA

[3]Department of Food Science and Technology, Department of Viticulture and Enology, University of California, Davis, CA, USA

[4]Department of Pathology, Harbor UCLA Medical Center, Torrance, CA, USA

[5]Department of Pathology and Laboratory Medicine, David Geffen School of Medicine, University of California, Los Angeles, CA, USA

Abstract

Dysregulated bile acid (BA) synthesis or reduced farnesoid X receptor (FXR) levels are found in patients having metabolic diseases, autoimmune hepatitis, and liver cirrhosis or cancer. The objective of this study was to establish the relationship between butyrate and dysregulated BA synthesis-induced hepatitis as well as the effect of butyrate in reversing the liver pathology. Wild-type (WT) and FXR knockout (KO) male mice were placed on a control (CD) or western diet (WD) for 15 months. In the presence or absence of butyrate supplementation, feces obtained from 15-month-old WD-fed FXR KO mice, which had severe hepatitis and liver tumors, were transplanted to 7-month-old WD-fed FXR KO for 3 months. Hepatic phenotypes, microbiota profile, and BA composition were analyzed. Butyrate-generating bacteria and colonic butyrate concentration were reduced due to FXR inactivation and further reduced by WD intake. In addition, WD-fed FXR KO male mice had the highest concentration of hepatic β-muricholic acid (β-MCA) and bacteria-generated deoxycholic acid (DCA) accompanied by serious hepatitis. Moreover, dysregulated BA and reduced SCFA signaling co-existed in both human liver cancers and WD-fed FXR KO mice. Microbiota transplantation using butyrate-deficient feces derived

*Correspondence to: Yu-Jui Yvonne Wan, PhD, Room 3400B, Research Building III, Department of Medical Pathology and Laboratory Medicine, University of California, Davis Health Systems, 4645 2nd Ave, Sacramento, CA 95817, USA. yjywan@ucdavis.edu.

Yu-Jui Yvonne Wan http://orcid.org/0000-0003-2243-7759

†These authors contributed equally to this work.

No conflicts of interest were declared.

Author contributions statement

YJW designed and supervised the implementation of the study. LS, PKJ, YH, HL, NN, and KMK performed experiments. LS, PKJ, YH, HL, NN, KMK, SWF (Harbor Medical Center), SWF (UCLA), DAM, and YJW analyzed and interpreted the data. LS, PKJ, and YJW wrote the manuscript. All authors commented on and approved the final manuscript.

from 15-month-old WD-fed FXR KO mice increased hepatic lymphocyte numbers as well as hepatic β-MCA and DCA concentrations. Furthermore, butyrate supplementation reduced hepatic β-MCA as well as DCA and eliminated hepatic lymphocyte infiltration. In conclusion, reduced butyrate contributes to the development of hepatitis in the FXR KO mouse model. In addition, butyrate reverses dysregulated BA synthesis and its associated hepatitis.

Keywords

short-chain fatty acids; hepatitis; liver cancer; gut microbiota; probiotics; FXR

Introduction

Dysregulated bile acid (BA) synthesis is implicated in the development of metabolic disease, autoimmune hepatitis, hepatic cirrhosis, and liver cancer [1–4]. Moreover, patients who have severe liver cirrhosis or cancer have reduced BA receptor, farnesoid X receptor (FXR) [5,6]. Consistently, FXR knockout (KO) mice that have dysregulated BA synthesis develop hepatitis and liver cancer spontaneously, and using cholestyramine to deplete BAs prohibits hepatic tumorigenesis in FXR KO mice [7–11]. In contrast to the whole body FXR KO mice, hepatocyte-specific FXR KO mice do not spontaneously develop liver cancer, and intestinal FXR KO mice are protected from diet-induced obesity and fatty liver [12–14]. These findings clearly indicate the significance of BAs and their receptor, FXR, in the liver and gut in controlling hepatic health and disease process [1–4,7,15–20].

BAs are generated jointly by hepatic and bacterial enzymes. In addition to hepatic enzymes that produce free and conjugated primary BAs, bile salt hydrolase found in *Bifidobacterium* and *Lactobacillus* deconjugates BAs, while 7α-dehydroxylase from the Firmicutes phylum converts primary BAs into secondary BAs [3,21]. Thus, BAs are not just detergents that are responsible for lipid absorption and metabolism; BAs are bacteria-generated metabolites that have pivotal roles in regulating inflammatory signaling and immunity [13,14,22,23]. However, the interaction between BAs and other bacterial metabolites remains to be investigated. The current study examines the effect of bacteria-generated butyrate in the development of hepatitis induced by dysregulated BAs in FXR KO mice as well as its effect in normalizing dysregulated BA-associated hepatitis.

The liver receives 70% of its blood supply from the intestine and is constantly exposed to intestinal-derived metabolites. Therefore, gut-derived signaling has a significant impact on liver pathology [4,24]. Commensal Gram-positive microbiota generates short-chain fatty acids (SCFAs) via fermentation of indigestible fibers. These SCFAs are not only important for gut but also affect the function of peripheral tissues. The detection of SCFA receptors, FFAR3 (GPR41), FFAR2 (GPR43), and HCAR2 (GPR109A), in adipose tissue, skeletal muscle, and liver implicates the involvement of SCFAs in peripheral tissues. Among the SCFAs, butyrate has an apparent histone deacetylase (HDAC) inhibitory property that is used to combat cancer [25,26]. Butyrate is also an energy source for colonocytes, and it increases tight junction proteins to reduce gut permeability [27]. Moreover, butyrate has anti-inflammatory as well as apoptotic effects and has been shown to be effective in colon

cancer prevention as well as treatment [28]. However, the hepatic concentration of butyrate is very low. The role of butyrate in liver disease development and prevention remains to be studied.

The current study examines the relationship between dysregulated BA synthesis and butyrate signaling. Our novel findings revealed that FXR KO mice had reduced butyrate-generating bacteria and western diet (WD) intake further decreased them. In addition, hepatitis can be induced through oral microbiota transplantation of butyrate-deficient feces. Furthermore, butyrate supplementation prevented hepatitis induced by dysregulated BA synthesis. Moreover, our novel data revealed that dysregulated BA and reduced SCFA signaling co-exist in human hepatocellular carcinoma aswell as in WD-fed FXR KO mice.

Materials and methods

Mice

C57BL/6 wild-type (WT) (Jackson Laboratory, Sacramento, CA, USA) and whole body FXR KO male mice [29] were given a WD (21% fat, 34% sucrose, and 0.2% cholesterol, w/w) or control diet (CD; 5% fat, 12% sucrose, and 0.01% cholesterol, w/w) from Harlan Teklad (Indianapolis, IN, USA) after weaning (3 weeks) and were euthanized at the age of 15 months. Experiments were conducted under protocols approved by the Institutional Animal Care and Use Committee of the University of California, Davis.

Fecal microbiota transplantation (FMT) and butyrate supplementation

Feces were collected from 15-month-old WD-fed FXR KO male mice. Fresh feces obtained from six mice were pooled in sterile phosphate-buffered saline (PBS). For FMT, 7-month-old WD-fed FXR KO male mice received PBS (control group) or pooled fecal material (30 mg feces/200 μl, FMT group) by oral gavage once a week for 3 months. Additionally, both control and FMT groups were divided into two sub-groups receiving or not receiving sodium butyrate (1 g/kg body weight via oral gavage, once a week for 3 months). Mice were euthanized when they were 10 months old.

Human specimens

Frozen liver cancer and normal livers, as confirmed by histological evaluation, were obtained from the Translational Pathology Core Laboratory Shared Resource at University of California, Los Angeles (UCLA). The tissue procurement process was approved by the UCLA Institutional Review Board with protocol number 11-2504 approved on 1 February 2011.

Quantification of bile acids

Liver tissue (50–100 mg) was collected from fed-state mice with gallbladder removed following BA extraction [30]. Hepatic BAs were quantified using a Prominence™ UFLC system (Shimadzu, Kyoto, Japan) coupled to an API 4000 QTRAP™ mass spectrometer (ABSciex, Redwood City, CA, USA) operated in the negative ionization mode. Chromatography was performed on a Kinetex C18 column (50 mm × 2.1 mm, 2.6 μm)

maintained at 40°C preceded by a high-pressure column pre-filter. The mobile phase consisted of a methanol gradient delivered at a flow rate of 0.4 ml/min [16,31,32].

Gene expression profiling

RNA was extracted using TRIzol Reagent (Invitrogen, Carlsbad, CA, USA), and cDNA was synthesized by reverse transcription (RT) using a High Capacity RNA-to-cDNA Kit (Applied Biosystems, Foster City, CA, USA). Quantitative PCR (qPCR) was performed on an ABI 7900HT Fast Real-time PCR system using Power SYBR® Green PCR Master Mix (Applied Biosystems). Primers were designed using Primer3 Input Software (v0.4.0) and are listed in the supplementary material, Table S1. The mRNA levels were normalized to the level of *Gapdh* mRNA.

Sample preparation and ^{1}H-NMR spectroscopic analysis

Colon contents (50–60 mg) were mixed with pre-cooled Na–K phosphate buffer and prepared according to the published method [33]. All ^{1}H-NMR data were collected on a Bruker AVANCE 600 Spectrometer (Bruker BioSpin, Rheinstetten, Germany). The samples were pre-cooled to 277 K before being loaded into the magnet, and warmed to 298 K and equilibrated for 5 min before data acquisition. A solvent pre-saturation pulse sequence was used to suppress the water signal. The data size was 64k and the relaxation delay was 2 s. A total of 64 scans were used to average out the signal and eight dummy scans were used before the acquisition pulse. Identification and quantification of metabolites were accomplished using Chenomx NMR Suite 7.6 (Chenomx, Inc, Edmonton, Alberta, Canada).

Quantification of proteins

Hepatic protein lysates (40 mg) were subjected to polyacrylamide gel electrophoresis under reducing conditions followed by transfer to polyvinylidene difluoride membranes. The membranes were incubated with 5% non-fat milk followed by an antibody. The following primary antibodies (catalogue number and dilutions) were used: TNF (AMC3812, 1:1000; Biosource International, Camarillo, CA, USA), TIMP1 (sc-5538, 1:200; Santa Cruz Biotechnology, Santa Cruz, CA, USA), IL6 (16-7061-81, 1:1000; eBioscience, San Diego, CA, USA), ACTA2 (1184-1, 1:1000; Epitomics, Burlingame, CA, USA), CCNA2 (NBP1-31330, 1:1000; Novus Biologicals, Littleton, CO, USA), p38 (9212, 1:1000; Cell Signaling Technology, Danvers, MA, USA), phosphorylated (p-) p38 (4551, 1:1000; Cell Signaling Technology), ERK1/2 (9102, 1:1000; Cell Signaling Technology), p-ERK1/2 (9101, 1:1000; Cell Signaling Technology), JNK (9252, 1:1000; Cell Signaling Technology), p-JNK (9251, 1:1000; Cell Signaling Technology), and β-actin (A1978, 1:10 000; Sigma Chemical Co, St Louis, MO, USA). Membranes were then incubated with horseradish peroxidase-conjugated secondary antibodies. The signals were detected using an ECL enhanced chemiluminescence system with Pierce SuperSignal West Pico chemiluminescent substrates (Thermo Fisher Scientific, Rockford, IL, USA).

Quantification of bacterial DNA and 16S rRNA gene sequencing

DNA was extracted from 0.1 g fecal samples using a ZR Fecal DNA MiniPrep Kit (Zymo Research, Irvine, CA, USA), quantified by a NanoDrop 8000 (Thermo Fisher Scientific),

and amplified using primers based on published sequences [34–36] (supplementary material, Table S2). A dissociation step was included to analyze the melting profile of amplified products. In parallel, qPCR was carried out using ten-fold serial diluted synthetic DNA fragments of a bacterial gene with known concentrations. Bacterial DNA concentration was calculated using standard curves of diluted synthetic DNA fragments. Sequencing of tagged 16S rRNA gene amplicons of fecal DNA was carried out based on published methods [37]. The V4 region of the 16S rRNA gene was amplified and sequenced using Illumina MiSeq.

Bioinformatics and statistical analysis

Sequence reads were analyzed using QIIME software. Spearman's correlations were performed with R Statistical Software. Data are expressed as mean ± SD. Differences between groups in microbiota family level were calculated using a Kruskal–Wallis test. All other comparisons were calculated using two-tailed Student's *t*-tests or one-way ANOVA followed by Tukey's test within GraphPad Prism 6 software (GraphPad Software, Inc, La Jolla, CA, USA). *P* values were adjusted formultiple comparisons using a false discovery rate. $P < 0.05$ was considered statistically significant.

Results

Hepatitis and tumor formation in WD-fed FXR KO mice

When mice were 15 months old, both WD-fed WT and CD-fed FXR KO male mice had hepatitis (Figure 1A and supplementary material, Figure S1A). However, only WD-fed FXR KO mice had grossly visible tumors (Figure 1A and supplementary material, Figure S1B). Hepatocellular carcinomas (HCCs), focal fatty change, bile duct adenoma, and hepatocellular adenoma were noted in WD-fed FXR KO mice (supplementary material, Figure S1B). WD intake increased the body weight and caused hepatomegaly in both WT and FXR KO mice (Figure 1B, C). Serum lipopolysaccharide (LPS) concentration was higher in FXR KO mice than in WT mice when they consumed a WD (Figure 1D). Additionally, flow cytometry data revealed that WD-fed FXR KO mice had substantially increased splenic TNF macrophage abundance, indicating systemic inflammation (Figure 1E).

The effect of diet and FXR status on hepatic and gut inflammatory signaling

WD and FXR inactivation significantly increased the hepatic mRNA levels of chemokine ligand 17 (*Ccl17*), ligand 20 (*Ccl20*), and ligand 2 (*Ccl2*), and WD-fed FXR KO mice had the highest levels (Figure 2A). Consistently, those genes are also highly induced in human HCC specimens [38–40]. WD intake and FXR deficiency also induced many other hepatic inflammatory genes, including *Tnf* (tumor necrosis factor), *Timp1* (tissue inhibitor of metalloproteinases), and *Icam1* (intercellular adhesion molecule 1). In addition, WD-fed FXR KOmice had the highest expression level ofmacrophage surface marker *Adgre1* (*F4/80*) and T-cell *Cd4* (supplementary material, Figure S2A). The markers of myofibroblasts including alpha-actin-2 (*Acta2*) and collagen type I alpha 1 (*Col1a1*) were also induced by WD intake and FXR deficiency, indicating the presence of an inflammation-driven fibrotic process (Figure 2A). Moreover, the increased *Ccna2* (cyclin A2) mRNA was found in both WD-fed and FXR KO mice, and WD-fed FXR KO mice had the highest *Ccna2* mRNA level,

implying increased proliferation. Moreover, the mRNA levels of SCFA receptors, i.e. *Ffar3*, *Frar2*, and *Hcar2*, were reduced in WD-fed FXR KO mice (Figure 2A).

In the colon, increased expression of inflammatory genes, *Ccl2*, *Il6*, *Nf-κB*, and surface markers for inflammatory cells [*Itgam* (*Cd11b*), *Cd8a*, and *Cd19*] was apparent in WD-fed FXR KO mice (Figure 2B and supplementary material, Figure S2B). In addition, both WD intake and FXR inactivation reduced the mRNA levels of tight junction genes including *Jam* (junction adhesion molecule), *Ocln* (occludin), and *Tjp1* (tight junction protein 1), suggesting increased gut permeability in WD-fed FXR KO mice. Furthermore, consistent with the data generated in the liver, the colonic mRNA levels of SCFA receptor genes were reduced due to WD intake as well as FXR deficiency.

Gut dysbiosis and reduced butyrate production caused by WD intake and FXR deficiency

FXR inactivation significantly reduced the abundance of Firmicutes, but increased Proteobacteria and Bacteroidetes (Figure 3A). In contrast, WD intake increased the abundance of Firmicutes, but reduced Bacteroidetes in both WT and FXR KO mice (Figure 3A). Additionally, the *Erysipelotrichaceae* family under Firmicutes, known as butyrate-generating bacteria, was substantially reduced from 65% to less than 2%, due to lack of FXR (Figure 3B). Moreover, there was an impressive increase of *Desulfovibrionaceae* and *Bacteroidaceae*, which rose from 1% in WT mice to 10% in FXR KO mice. Furthermore, quantification of fecal bacterial genes revealed that FXR inactivation reduced the abundance of the butyrate-producing gene *bcoA* (butyryl-CoA:acetate CoA transferase) [35,36], which was further reduced by WD intake (Figure 3C). Conversely, the abundance of the secondary BA-generating gene *baiJ* [34] was increased by FXR inactivation and further increased by WD feeding (Figure 3C). Consistent with bacterial gene abundance data, the concentration of colonic butyrate was lowest in WD-fed FXR KO mice (Figure 3D). Moreover, there was a positive and significant correlated relationship between the abundance of *Erysipelotrichaceae* and colon butyrate concentration ($r = 0.6586$, $p = 0.0016$), as well as the abundance of *Desulfovibrionaceae* and serum endotoxin LPS level ($r = 0.6651$, $p = 0.0014$) (Figure 3E).

Reduced expression of FXR and SCFA receptor genes in human HCC specimens

To understand the significance of FXR and SCFA signaling in liver cancers, the expression of *FXR* and its target as well as SCFA receptor genes was studied in 14 HCCs and 14 normal liver tissues, of which ten pairs were derived from HCC (T) and adjacent normal tissues (N) of ten patients. Among the 14 HCC patients, six had HBV, of which one also had a moderate alcohol drinking history (up to two drinks per day). Three patients had HCV, of which one patient also had steatosis. Among the other five patients, who did not have viral infection, three had steatosis or non-alcoholic steatohepatitis, and another patient had a moderate alcohol drinking history. One patient had no history of steatosis or drinking. Thus, regardless of the etiology of HCCs, cancer specimens had reduced *FXR* and FXR direct target gene *SHP*, but increased *CCNA2* mRNA level (Figure 4A). Additionally, our novel data revealed that HCCs had reduced expression of SCFA receptors, *FFAR3*, *FFAR2*, and *HCAR2* (Figure 4A). These findings suggest the significant role of FXR as well as SCFA signaling in protecting the health of human livers.

Increased expression of SCFA receptor genes and reduced hepatic inflammatory genes due to butyrate supplementation

To study the effect of butyrate *in vivo*, WT mice were fed with butyrate (1 g/kg body weight) by oral gavage daily for 7 days. Butyrate increased the mRNA levels of SCFA receptor genes in the colon (Figure 4B). In addition, butyrate reduced colonic *Il6*, but increased the expression of tight junction genes, i.e. *Tjp1*, *Ocln*, and *Jam* (Figure 4B). Moreover, butyrate markedly reduced the expression of hepatic inflammation genes including *Ccl17*, *Ccl20*, *Ccl2*, *Tnf*, *Timp1*, and *Il6* (Figure 4C). Furthermore, butyrate intake reduced hepatic *Col1a1* and *Acta2* as well as *Ccna2*, which was opposite to WD intake and lack of FXR shown in Figure 2. The expression level of key hepatic metabolic regulators, i.e. *Pparα* (peroxisome proliferator-activated receptor α) and *Pgc-1α* (PPARγ coactivator 1α), was also induced by butyrate. Consistently, butyrate reduced hepatic TNF, TIMP1, IL6, ACTA2, and CCNA2 protein levels (Figure 4D). Together, butyrate exerts anti-inflammatory effects in the liver and colon.

The effect of butyrate-deficient feces and butyrate supplementation on the development of hepatitis

Because WD-fed FXR KO male mice had the most severe hepatic inflammation, the feces of 15-month-old male WD-fed FXR KO mice, which lacked butyrate-generating bacteria, were orally transplanted to 7-month-old male WD-fed FXR KO mice with or without butyrate supplementation. The transplantation was conducted once a week and hepatic lymphocyte infiltration increased after 3months of FMT (Figure 5A, B). Butyrate supplementation increased colon butyrate concentration (Figure 5C). In addition, butyrate supplementation abolished hepatic lymphocyte infiltration and reduced steatosis in mice with and without FMT (Figure 5A, B and supplementary material, Figure S3). Consistent with the morphological data, FMT increased the expression of hepatic inflammatory genes as well as surface markers for different types of inflammatory cells [*Ptprc* (*Cd45*), *Adgre1* (*F4/80*), *Itgax* (*Cd11c*), *Cd4*, and *Cd8a*], but reduced SCFA receptor genes. Additionally, butyrate intake reversed those changes (Figure 5D and supplementary material, Figure S4A). Western blot analysis showed that FMT increased hepatic protein levels of TNF and IL6, which were reduced by butyrate (Figure 5E).

Hepatic pathway analysis revealed that transplantation of butyrate-deficient feces reduced the total p38 level, but butyrate increased the total as well as p-p38. In addition, butyrate reduced p-ERK1/2, but FMT of butyrate-deficient feces did not seem to influence total or p-ERK1/2. Moreover, total JNK and p-JNK were not changed by FMT or butyrate treatment (Figure 5F).

In the colon, FMT reduced the expression of tight junction as well as SCFA receptor genes, but increased pro-inflammatory genes (*Il6*, *Tnf*, and *Nf-κB*) and most studied surface markers of inflammatory cells. Moreover, butyrate was also able to reverse those changes that occurred in the gut (Figure 5G and supplementary material, Figure S4B).

Hepatic BAs affected by WD intake, FXR deactivation, fecal transplantation, and butyrate supplementation

Both WD intake and FXR deficiency altered the concentration of hepatic total as well as individual BAs (Figure 6A). Free β-muricholic acid (β-MCA) had the largest fold increase due to WD intake and lack of FXR when mice were 15 months old (Figure 6A). The toxic secondary BA, deoxycholic acid (DCA), also had a steady increase due to WD intake and FXR KO, and WD-fed FXR KO had the highest hepatic DCA concentration (Figure 6A). The pattern of change of hyodeoxycholic acid (HDCA) was similar to that of DCA. The changes of other BAs are shown in the supplementary material, Figure S5.

Butyrate treatment did not change total hepatic BA and HDCA concentration (Figure 6B). However, butyrate supplementation reduced FMT-increased β-MCA and DCA (Figure 6B). Those changes were also consistent with the shift in the abundance of bacterial gene *baiJ* (Figure 6C). In addition, butyrate did not cause a significant change for other BAs (data not shown). Furthermore, correlation analysis revealed that the concentrations of hepatic β-MCA and DCA were negatively correlated with colonic butyrate concentration ($r = -0.4582$, $p = 0.0084$ and $r = -0.4627$, $p = 0.0077$, respectively), but were positively associated with serum LPS level ($r = 0.6533$, $p < 0.0001$ and $r = 0.5778$, $p = 0.0005$, respectively) in both 15-month-old and FMT mice (Figure 6D).

Discussion

This study revealed for the first time that reduced butyrate-generating bacteria as well as SCFA signaling is associated with deactivation of FXR and WD intake-induced hepatitis. Microbiota transplantation using feces that lack butyrate-generating bacteria increased hepatic inflammation. Additionally, butyrate intake abolished hepatic inflammation caused by FXR inactivation-associated dysregulated BA synthesis. The significance of BA dysregulation in contributing to liver diseases has been revealed [1–4]. Our novel data showed that butyrate can reverse some of the most significant changes in BA production caused by WD intake and FXR inactivation as well as their associated pathology, i.e. hepatic inflammation. These findings clearly indicate the importance of butyrate as well as butyrate-generating bacteria in maintaining liver health, which has not been established before.

The potential effect of butyrate in the liver

Butyrate is present in dietary products such as cottage cheese. In addition, butyrate and other SCFAs are produced by fermentation of indigestible fibers in the gut. Among acetate, butyrate, and propionate, butyrate supplies ~60–70% of the energy required by colonocytes, and butyrate plays a key role in maintaining gut epithelial integrity [41]. Butyrate, together with acetate and propionate, can transfer from the gut and be used by the liver [42]. Butyrate is metabolized directly by the hepatocytes [43]. Thus, the effect of butyrate on hepatic inflammatory and metabolic signaling can be direct or secondary through improving gut health. It is also possible that increased butyrate may change the concentration of acetate and propionate, which in turn affects liver health. Those possibilities warrant further investigation.

Among the three SCFA receptors, HCAR2 is butyrate and niacin-specific. FFAR3 is preferentially activated by propionate followed by butyrate and acetate, while FFAR2 can be activated by all three SCFAs [41]. Our novel data showed that the expression of all three SCFA receptors was reduced in the liver and gut of WD-fed FXR KO mice, indicating an interactive effect between dysregulated BA synthesis and SCFA signaling. Additionally, our data for the first time revealed that butyrate intake increased the expression of all three SCFA receptor genes in the gut, which was correlated with reduced inflammation in the gut and liver. These findings suggested that butyrate might be able to increase acetate as well as propionate signaling. Consistent with animal models, data generated using clinical specimens revealed that HCC specimens also have reduced SCFA receptors as well as FXR signaling, again linking these two signaling pathways together. Butyrate potentially can be used for colon cancer prevention and treatment [28]. The effect of SCFAs in liver cancer prevention and treatment should be explored.

The anti-inflammatory effect of butyrate is in part due to its ability to increase the expression of tight junction and prevent leaky gut. Its beneficial effect can also be due to increased metabolism that reduces oxidative stress. Additionally, butyrate has an HDAC inhibitory property, which reduces inflammation through epigenetic mechanisms [25]. Moreover, butyrate has anti-inflammatory effects in monocytes, macrophages, osteoblasts, or skin tissue via ERK1/2 deactivation [44–48]. Furthermore, butyrate activates p38, which may contribute to increased PGC-1α activity [49,50]. Consistently, our data revealed that butyrate intake increased both total and activated p38. Our data also suggested that dysregulated BA synthesis may contribute to hepatic p38 deactivation.

Gut dysbiosis and hepatic inflammation

The reduced relative abundance of *Erysipelotrichaceae* (from 65% to 2%) and increased *Bacteroidaceae* (from 1% to 10%) can account for the substantial change of Firmicutes and Bacteroidetes, respectively. *Erysipelotrichaceae* is involved in BA deconjugation and butyrate production [51,52]. Reduced *Erysipelotrichaceae* was found in patients with Crohn's disease [53]. In addition, there was a strong positive correlation between butyrate concentration and *Erysipelotrichaceae* abundance, suggesting the impact of *Erysipelotrichaceae* on hepatic inflammation. However, reduction of *Erysipelotrichaceae* was FXR deficiency-specific because WD intake did not further reduce the abundance of *Erysipelotrichaceae*. Thus, there might be other butyrate-generating bacteria that account for the reduced *bcoA* and colonic butyrate concentration in WD-fed mice. In addition, the increased abundance of the *Desulfovibrionaceae* family, which generates hydrogen sulfide, a genotoxin and mucosal barrier-breaker, was positively correlated with serum LPS level in FXR KO mice [54,55]. Moreover, the enriched *Bacteroidaceae* in FXR KO mice might increase the risk for development of intestinal inflammation [56]. Those findings may in part explain the systemic inflammation found in WD-fed FXR KO mice. Furthermore, WD-fed FXR KO mice had an increased abundance of secondary BA-generating *baiJ* in the fecal microbiota. Transplantation of butyrate-deficient feces led to an increased abundance of *baiJ*, while butyrate supplementation reduced it. These findings were also consistent with the changes of hepatic secondary DCA level. Together, the abundance of butyrate and secondary BA-generating bacteria is inversely correlated.

Bile acid synthesis dysregulation and liver health

Hepatic total BA was increased due to WD intake and FXR deficiency. However, fecal transplantation of butyrate-deficient feces, which increased hepatic lymphocyte infiltration, did not further increase hepatic total BA, indicating the significance of individual rather than total BA in causing hepatic inflammation. FXR inactivation-associated liver tumorigenesis can be prevented by using cholestyramine to deplete BAs [8]. The current study reveals the capability of butyrate in shifting individual BA levels such as DCA, which may be a realistic approach to prevent liver tumorigenesis.

A high concentration of fecal DCA is found in obese individuals [57]. DCA induces a senescence-associated secretory phenotype of the hepatic stellate cells, which secrete inflammatory and proliferative factors [34]. In addition, DCA has proliferative properties by inducing nuclear NUR77 [58]. However, HDAC inhibitors can induce cytosolic NUR77 expression, leading to cancer cell apoptosis [59]. Due to the HDAC inhibitory effect of butyrate, it is possible that butyrate increases cytosolic NUR77 and has an anti-tumor effect. It would be interesting to further study the effect of butyrate in other health conditions that have dysregulated BA synthesis such as primary biliary cholangitis and primary sclerosing cholangitis.

Both WD intake and FXR deficiency increased hepatic β-MCA, and WD-fed FXR KO male mice had the highest concentration of β-MCA. The increased concentration of β-MCA in WD-fed FXR KO mice could be reduced by butyrate supplementation. Moreover, our data showed that increased hepatic β-MCA was positively associated with serum LPS level but negatively correlated with butyrate concentration. It is important to note that β-MCA can be detected in human urine [60,61]. The regulatory mechanism of butyrate on hepatic β-MCA as well as the pathological and physiological impact of β-MCA warrants further investigation.

In conclusion, dysregulated BA synthesis-associated hepatic inflammation was accompanied by decreased butyrate-generating bacteria and reduced SCFA signaling, which can be reversed by butyrate supplementation. All of those changes are associated with shifts in BA profiles as well as BA-producing bacterial abundance. Thus, butyrate and BA-generating bacteria likely can affect each other’s growth and expansion. Dietary intervention as well as probiotic intake can potentially be used to treat and prevent liver diseases including HCC. This notion is supported by a study that shows that a combination of *Lactobacillus rhamnosus* GG, *Escherichia coli* Nissle 1917, and heat-inactivated VSL#3 reduces the size of HCC in xenograft models by increasing the SCFA level in the gut [62]. It would be important to test the effect of different strains of butyrate-generating bacteria on regulating the BA profile and liver cancer prevention and treatment in the future.

Supplementary Material

Refer to Web version on PubMed Central for supplementary material.

Acknowledgments

We thank Dr Frank J. Gonzalez at NCI for providing FXR KO mice and Niki Taylor DeGeorge for editing the manuscript. This work was supported by National Institutes of Health, Grant U01CA179582.

References

1. Li T, Chiang JY. Bile acids as metabolic regulators. Curr Opin Gastroenterol. 2015; 31:159–165. [PubMed: 25584736]
2. Li T, Chiang JY. Bile acid signaling in metabolic disease and drug therapy. Pharmacol Rev. 2014; 66:948–983. [PubMed: 25073467]
3. Lefebvre P, Cariou B, Lien F, et al. Role of bile acids and bile acid receptors in metabolic regulation. Physiol Rev. 2009; 89:147–191. [PubMed: 19126757]
4. Liu HX, Keane R, Sheng L, et al. Implications of microbiota and bile acid in liver injury and regeneration. J Hepatol. 2015; 63:1502–1510. [PubMed: 26256437]
5. Liu N, Meng Z, Lou G, et al. Hepatocarcinogenesis in $FXR^{-/-}$ mice mimics human HCC progression that operates through HNF1α regulation of FXR expression. Mol Endocrinol. 2012; 26:775–785. [PubMed: 22474109]
6. Su H, Ma C, Liu J, et al. Downregulation of nuclear receptor FXR is associated with multiple malignant clinicopathological characteristics in human hepatocellular carcinoma. Am J Physiol Gastrointest Liver Physiol. 2012; 303:G1245–G1253. [PubMed: 23042943]
7. Zhang Y, Ge X, Heemstra LA, et al. Loss of FXR protects against diet-induced obesity and accelerates liver carcinogenesis in ob/ob mice. Mol Endocrinol. 2012; 26:272–280. [PubMed: 22261820]
8. Yang F, Huang XF, Yi TS, et al. Spontaneous development of liver tumors in the absence of the bile acid receptor farnesoid X receptor. Cancer Res. 2007; 67:863–867. [PubMed: 17283114]
9. Kim I, Morimura K, Shah Y, et al. Spontaneous hepatocarcinogenesis in farnesoid X receptor-null mice. Carcinogenesis. 2007; 28:940–946. [PubMed: 17183066]
10. Li G, Kong B, Zhu Y, et al. Small heterodimer partner overexpression partially protects against liver tumor development in farnesoid X receptor knockout mice. Toxicol Appl Pharmacol. 2013; 272:299–305. [PubMed: 23811326]
11. Wolfe A, Thomas A, Edwards G, et al. Increased activation of the Wnt/beta-catenin pathway in spontaneous hepatocellular carcinoma observed in farnesoid X receptor knockout mice. J Pharmacol Exp Ther. 2011; 338:12–21. [PubMed: 21430080]
12. Kong B, Zhu Y, Li G, et al. Mice with hepatocyte-specific FXR deficiency are resistant to spontaneous but susceptible to cholic acid-induced hepatocarcinogenesis. Am J Physiol Gastrointest Liver Physiol. 2016; 310:G295–G302. [PubMed: 26744468]
13. Jiang CT, Xie C, Li F, et al. Intestinal farnesoid X receptor signaling promotes nonalcoholic fatty liver disease. J Clin Invest. 2015; 125:386–402. [PubMed: 25500885]
14. Li F, Jiang CT, Krausz KW, et al. Microbiome remodelling leads to inhibition of intestinal farnesoid X receptor signalling and decreased obesity. Nat Commun. 2013; 4:2384. [PubMed: 24064762]
15. Xu Y, Li F, Zalzala M, et al. Farnesoid X receptor activation increases reverse cholesterol transport by modulating bile acid composition and cholesterol absorption in mice. Hepatology. 2016; 64:1072–1085. [PubMed: 27359351]
16. Liu HX, Rocha CS, Dandekar S, et al. Functional analysis of the relationship between intestinal microbiota and the expression of hepatic genes and pathways during the course of liver regeneration. J Hepatol. 2016; 64:641–650. [PubMed: 26453969]
17. Huang XF, Zhao WY, Huang WD. FXR and liver carcinogenesis. Acta Pharmacol Sin. 2015; 36:37–43. [PubMed: 25500874]
18. Ma Y, Huang Y, Yan L, et al. Synthetic FXR agonist GW4064 prevents diet-induced hepatic steatosis and insulin resistance. Pharm Res. 2013; 30:1447–1457. [PubMed: 23371517]
19. de Aguiar Vallim TQ, Tarling EJ, Edwards PA. Pleiotropic roles of bile acids in metabolism. Cell Metab. 2013; 17:657–669. [PubMed: 23602448]

20. Modica S, Gadaleta RM, Moschetta A. Deciphering the nuclear bile acid receptor FXR paradigm. Nucl Recept Signal. 2010; 8:e005. [PubMed: 21383957]
21. Jones BV, Begley M, Hill C, et al. Functional and comparative metagenomic analysis of bile salt hydrolase activity in the human gut microbiome. Proc Natl Acad Sci U S A. 2008; 105:13580–13585. [PubMed: 18757757]
22. Parseus A, Sommer N, Sommer F, et al. Microbiota-induced obesity requires farnesoid X receptor. Gut. 2017; 66:429–437. [PubMed: 26740296]
23. Inagaki T, Moschetta A, Lee YK, et al. Regulation of antibacterial defense in the small intestine by the nuclear bile acid receptor. Proc Natl Acad Sci U S A. 2006; 103:3920–3925. [PubMed: 16473946]
24. Tsuei J, Chau T, Mills D, et al. Bile acid dysregulation, gut dysbiosis, and gastrointestinal cancer. Exp Biol Med. 2014; 239:1489–1504.
25. Davie JR. Inhibition of histone deacetylase activity by butyrate. J Nutr. 2003; 133:2485s–2493s. [PubMed: 12840228]
26. Donohoe DR, Holley D, Collins LB, et al. A gnotobiotic mouse model demonstrates that dietary fiber protects against colorectal tumorigenesis in a microbiota- and butyrate-dependent manner. Cancer Discov. 2014; 4:1387–1397. [PubMed: 25266735]
27. Canani RB, Costanzo MD, Leone L, et al. Potential beneficial effects of butyrate in intestinal and extraintestinal diseases. World J Gastroenterol. 2011; 17:1519–1528. [PubMed: 21472114]
28. Encarnacao JC, Abrantes AM, Pires AS, et al. Revisit dietary fiber on colorectal cancer: butyrate and its role on prevention and treatment. Cancer Metast Rev. 2015; 34:465–478.
29. Sinal CJ, Tohkin M, Miyata M, et al. Targeted disruption of the nuclear receptor FXR/BAR impairs bile acid and lipid homeostasis. Cell. 2000; 102:731–744. [PubMed: 11030617]
30. Garcia-Canaveras JC, Donato MT, Castell JV, et al. Targeted profiling of circulating and hepatic bile acids in human, mouse, and rat using a UPLC-MRM-MS-validated method. J Lipid Res. 2012; 53:2231–2241. [PubMed: 22822028]
31. Liu HX, Hu Y, Wan YJY. Microbiota and bile acid profiles in retinoic acid-primed mice that exhibit accelerated liver regeneration. Oncotarget. 2016; 7:1096–1106. [PubMed: 26701854]
32. Yang F, Hu Y, Liu HX, et al. MiR-22-silenced cyclin A expression in colon and liver cancer cells is regulated by bile acid receptor. J Biol Chem. 2015; 290:6507–6515. [PubMed: 25596928]
33. Tian Y, Zhang L, Wang Y, et al. Age-related topographical metabolic signatures for the rat gastrointestinal contents. J Proteome Res. 2012; 11:1397–1411. [PubMed: 22129435]
34. Yoshimoto S, Loo TM, Atarashi K, et al. Obesity-induced gut microbial metabolite promotes liver cancer through senescence secretome. Nature. 2013; 499:97–101. [PubMed: 23803760]
35. Louis P, Flint HJ. Development of a semiquantitative degenerate real-time PCR-based assay for estimation of numbers of butyryl-coenzyme A (CoA) CoA transferase genes in complex bacterial samples. Appl Environ Microbiol. 2007; 73:2009–2012. [PubMed: 17259367]
36. O'Keefe SJ, Li JV, Lahti L, et al. Fat, fibre and cancer risk in African Americans and rural Africans. Nat Commun. 2015; 6:6342. [PubMed: 25919227]
37. Frese SA, Parker K, Calvert CC, et al. Diet shapes the gut microbiome of pigs during nursing and weaning. Microbiome. 2015; 3:28. [PubMed: 26167280]
38. Zhu F, Li X, Chen S, et al. Tumor-associated macrophage or chemokine ligand CCL17 positively regulates the tumorigenesis of hepatocellular carcinoma. Med Oncol. 2016; 33:17. [PubMed: 26781124]
39. Ding X, Wang K, Wang H, et al. High expression of CCL20 is associated with poor prognosis in patients with hepatocellular carcinoma after curative resection. J Gastrointest Surg. 2012; 16:828–836. [PubMed: 22072303]
40. Wang WW, Ang SF, Kumar R, et al. Identification of serum monocyte chemoattractant protein-1 and prolactin as potential tumor markers in hepatocellular carcinoma. PLoS One. 2013; 8:e68904. [PubMed: 23874805]
41. Canfora EE, Jocken JW, Blaak EE. Short-chain fatty acids in control of body weight and insulin sensitivity. Nat Rev Endocrinol. 2015; 11:577–591. [PubMed: 26260141]

42. Bloemen JG, Venema K, van de Poll MC, et al. Short chain fatty acids exchange across the gut and liver in humans measured at surgery. Clin Nutr. 2009; 28:657–661. [PubMed: 19523724]
43. den Besten G, van Eunen K, Groen AK, et al. The role of short-chain fatty acids in the interplay between diet, gut microbiota, and host energy metabolism. J Lipid Res. 2013; 54:2325–2340. [PubMed: 23821742]
44. Park JS, Lee EJ, Lee JC, et al. Anti-inflammatory effects of short chain fatty acids in IFN-gamma-stimulated RAW 264.7 murine macrophage cells: involvement of NF-kappaB and ERK signaling pathways. Int Immunopharmacol. 2007; 7:70–77. [PubMed: 17161819]
45. Djouad F, Rackwitz L, Song Y, et al. ERK1/2 activation induced by inflammatory cytokines compromises effective host tissue integration of engineered cartilage. Tissue Eng Part A. 2009; 15:2825–2835. [PubMed: 19243242]
46. Seo SW, Lee D, Minematsu H, et al. Targeting extracellular signal-regulated kinase (ERK) signaling has therapeutic implications for inflammatory osteolysis. Bone. 2010; 46:695–702. [PubMed: 19895919]
47. Pastore S, Mascia F, Mariotti F, et al. ERK1/2 regulates epidermal chemokine expression and skin inflammation. J Immunol. 2005; 174:5047–5056. [PubMed: 15814736]
48. Kurosawa M, Numazawa S, Tani Y, et al. ERK signalingmediates the induction of inflammatory cytokines by bufalin in human monocytic cells. Am J Physiol Cell Physiol. 2000; 278:C500–C508. [PubMed: 10712238]
49. Witt O, Sand K, Pekrun A. Butyrate-induced erythroid differentiation of human K562 leukemia cells involves inhibition of ERK and activation of p38 MAP kinase pathways. Blood. 2000; 95:2391–2396. [PubMed: 10733512]
50. Gao Z, Yin J, Zhang J, et al. Butyrate improves insulin sensitivity and increases energy expenditure in mice. Diabetes. 2009; 58:1509–1517. [PubMed: 19366864]
51. Vital M, Howe AC, Tiedje JM. Revealing the bacterial butyrate synthesis pathways by analyzing (meta)genomic data. mBio. 2014; 5:e00889. [PubMed: 24757212]
52. Labbé A, Ganopolsky JG, Martoni CJ, et al. Bacterial bile metabolising gene abundance in Crohn's, ulcerative colitis and type 2 diabetes metagenomes. PLoS One. 2014; 9:e115175. [PubMed: 25517115]
53. Gevers D, Kugathasan S, Denson LA, et al. The treatment-naive microbiome in new-onset Crohn's disease. Cell Host Microbe. 2014; 15:382–392. [PubMed: 24629344]
54. Devkota S, Wang YW, Musch MW, et al. Dietary-fat-induced taurocholic acid promotes pathobiont expansion and colitis in *Il10*$^{-/-}$ mice. Nature. 2012; 487:104–108. [PubMed: 22722865]
55. Wei ZS, Augusto LA, Zhao LP, et al. *Desulfovibrio desulfuricans* isolates from the gut of a single individual: structural and biological lipid A characterization. FEBS Lett. 2015; 589:165–171. [PubMed: 25479086]
56. Schaubeck M, Clavel T, Calasan J, et al. Dysbiotic gut microbiota causes transmissible Crohn's disease-like ileitis independent of failure in antimicrobial defence. Gut. 2016; 65:225–237. [PubMed: 25887379]
57. Bernstein H, Bernstein C, Payne CM, et al. Bile acids as carcinogens in human gastrointestinal cancers. Mutat Res. 2005; 589:47–65. [PubMed: 15652226]
58. Hu Y, Chau T, Liu HX, et al. Bile acids regulate nuclear receptor (Nur77) expression and intracellular location to control proliferation and apoptosis. Mol Cancer Res. 2015; 13:281–292. [PubMed: 25232032]
59. Yang H, Zhan Q, Wan YJ. Enrichment of Nur77 mediated by retinoic acid receptor beta leads to apoptosis of human hepatocellular carcinoma cells induced by fenretinide and histone deacetylase inhibitors. Hepatology. 2011; 53:865–874. [PubMed: 21319187]
60. Goto J, Hasegawa K, Nambara T, et al. Studies on steroids. CCLIV. Gas chromatographic–mass spectrometric determination of 4- and 6-hydroxylated bile acids in human urine with negative ion chemical ionization detection. J Chromatogr. 1992; 574:1–7. [PubMed: 1629271]
61. Bathena SPR, Thakare R, Gautam N, et al. Urinary bile acids as biomarkers for liver diseases I. Stability of the baseline profile in healthy subjects. Toxicol Sci. 2015; 143:296–307. [PubMed: 25344562]

62. Li J, Sung CYJ, Lee N, et al. Probiotics modulated gut microbiota suppresses hepatocellular carcinoma growth in mice. Proc Natl Acad Sci U S A. 2016; 113:E1306–E1315. [PubMed: 26884164]

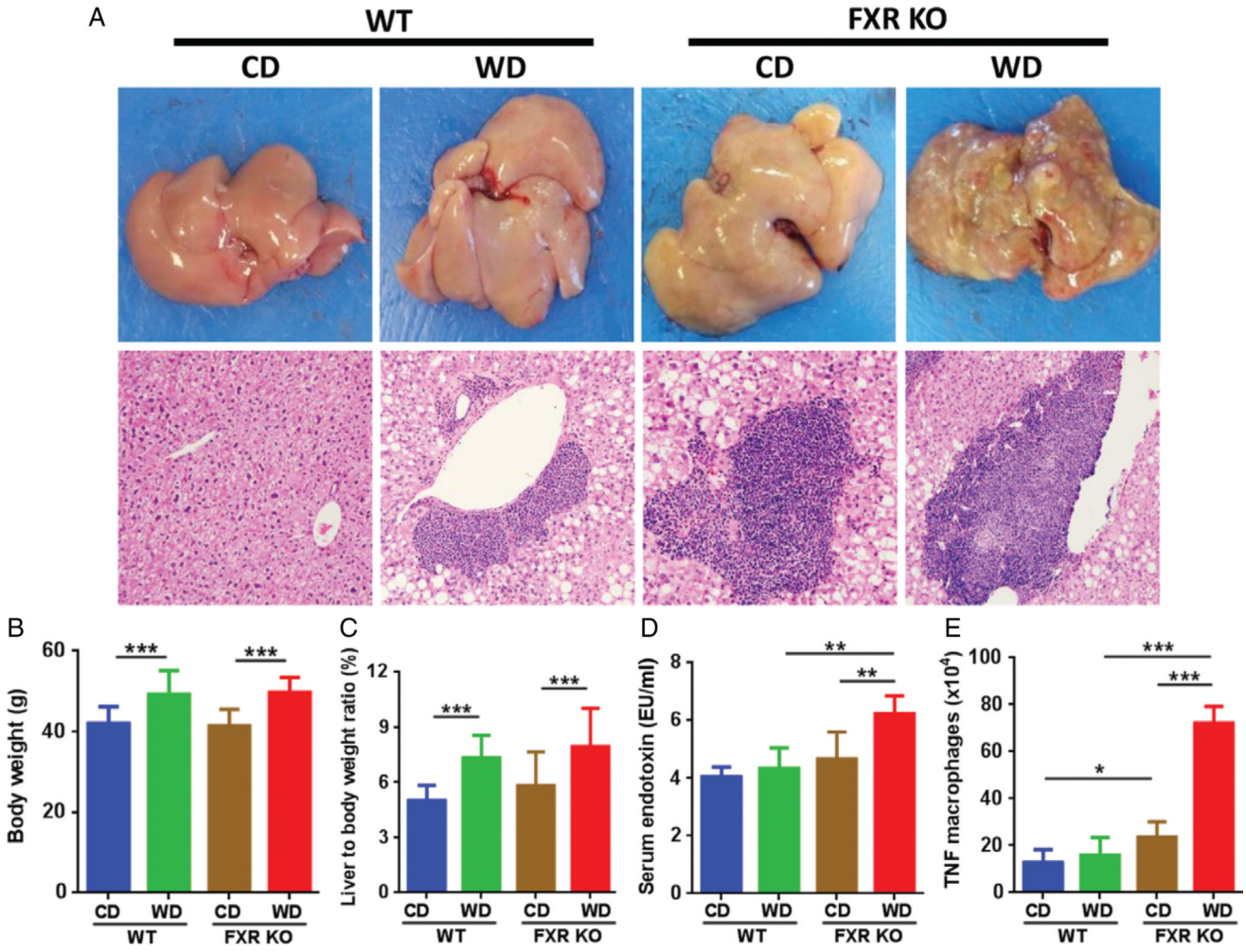

Figure 1.

Histological and phenotypic changes in control diet (CD) and western diet (WD)-fed wild-type and FXR KO mice. (A) Representative liver morphology and H&E-stained liver sections (original magnification 40×). (B) Body weight. (C) Percentage of liver to body weight ratio. (D) Serum endotoxin level. (E) Flow cytometric analysis of spleen TNF macrophages. $n = 8$ per group. Data are expressed as mean ± SD. One-way ANOVA with Tukey's correction. *$p < 0.05$; **$p < 0.01$; ***$p < 0.001$.

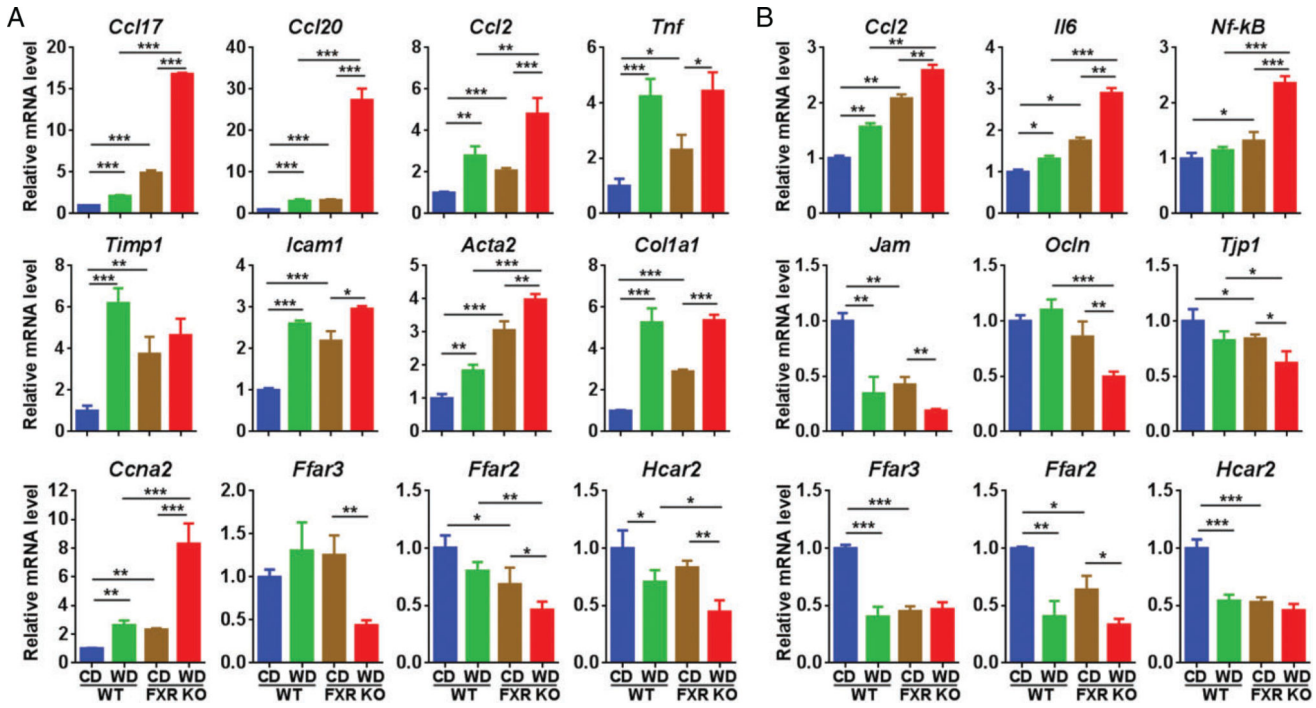

Figure 2.

Hepatic (A) and colon (B) gene expression in control diet (CD) and western diet (WD)-fed wild-type and FXR KO mice. $n = 8$ per group. Data are expressed as mean ± SD. One-way ANOVA with Tukey's correction. *$p < 0.05$; **$p < 0.01$; ***$p < 0.001$.

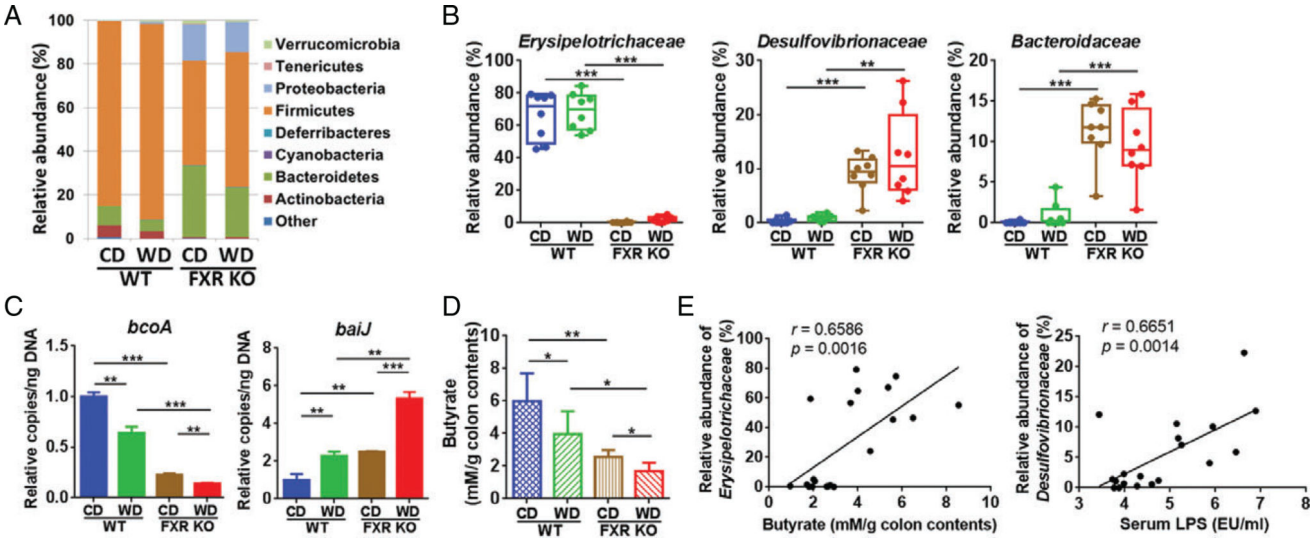

Figure 3.

Alteration of gutmicrobiota and butyrate concentration in control diet (CD) and western diet (WD)-fed wild-type and FXR KOmice. (A) Fecal microbiota changes at phylum level. (B) Relative abundance of fecal microbiota changes at family level. (C) Targeted functional quantitative PCR analysis of microbial genes. Copy number per ng DNA was calculated in each group and the relative changes to CD-fed WT mice are shown. $n = 8$ per group. (D) NMR analysis of butyrate concentration in colon contents. $n = 5$ per group. (E) Correlation between *Erysipelotrichaceae* abundance and butyrate concentration in the colon contents, as well as *Desulfovibrionaceae* abundance and serum endotoxin LPS. Each dot represents one mouse. The straight line represents the best-fit line obtained by linear regression analysis. *$p < 0.05$; **$p < 0.01$; ***$p < 0.001$.

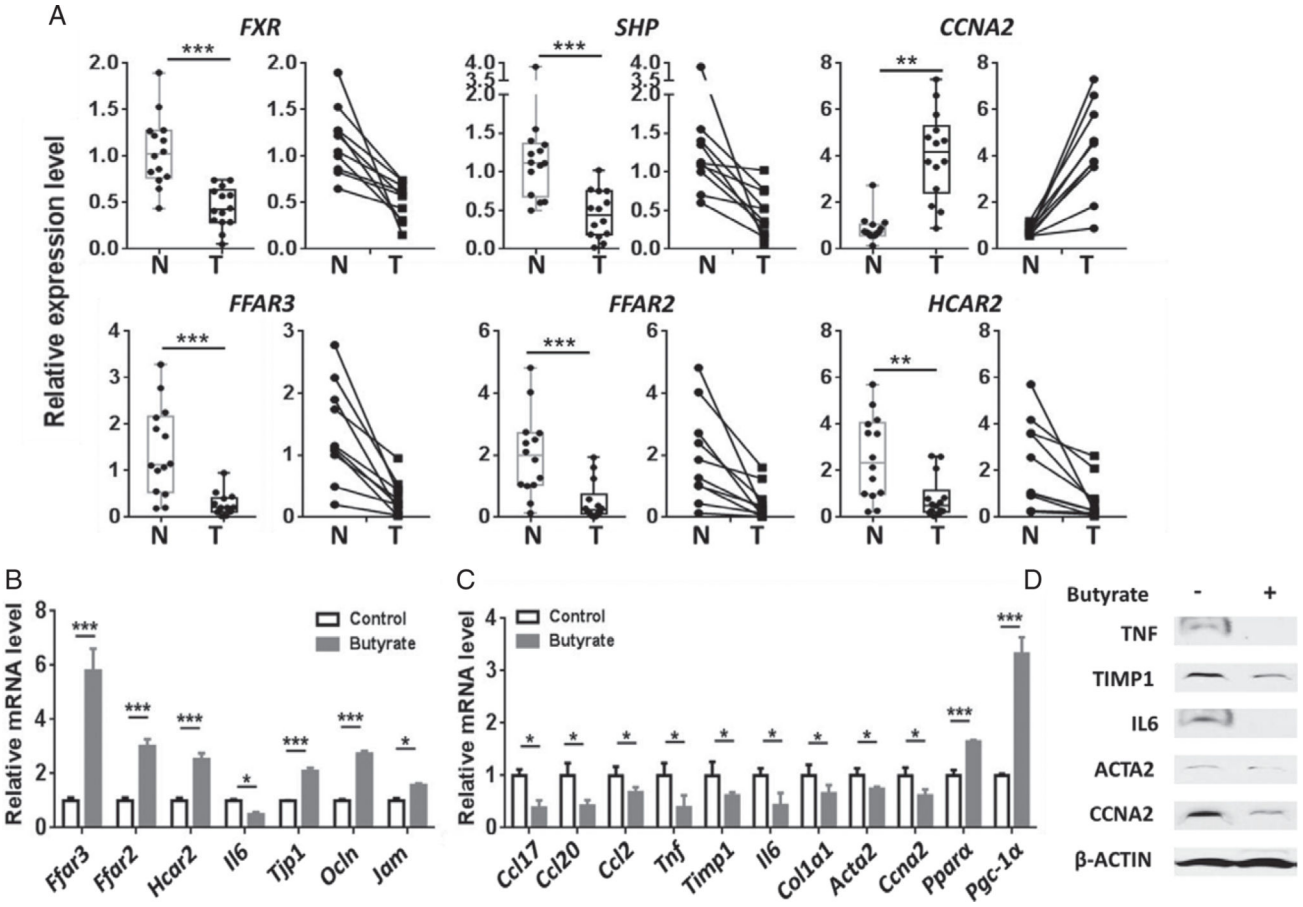

Figure 4.

Gene expression in human normal livers and HCC specimens as well as in wild-type male mice with and without butyrate supplementation. (A) The mRNA level of genes involved in the FXR signaling pathway and SCFA receptors in HCCs (T, $n = 14$) and normal liver tissues (N, $n = 14$) (left figure for each gene). In the 28 liver specimens studied, ten pairs were derived from HCC and adjacent normal tissues of the same patients (right figure for each gene). Colonic (B) and hepatic (C) gene expression in 2-month-old wild-type male mice with and without sodium butyrate supplementation (1 g/kg body weight, oral gavage, daily for 7 days). $n = 4$ per group. (D) Hepatic protein levels of the same mice described in C. Data are expressed as mean ± SD. Two-tailed Student's *t*-test. *$p < 0.05$; **$p < 0.01$; ***$p < 0.001$.

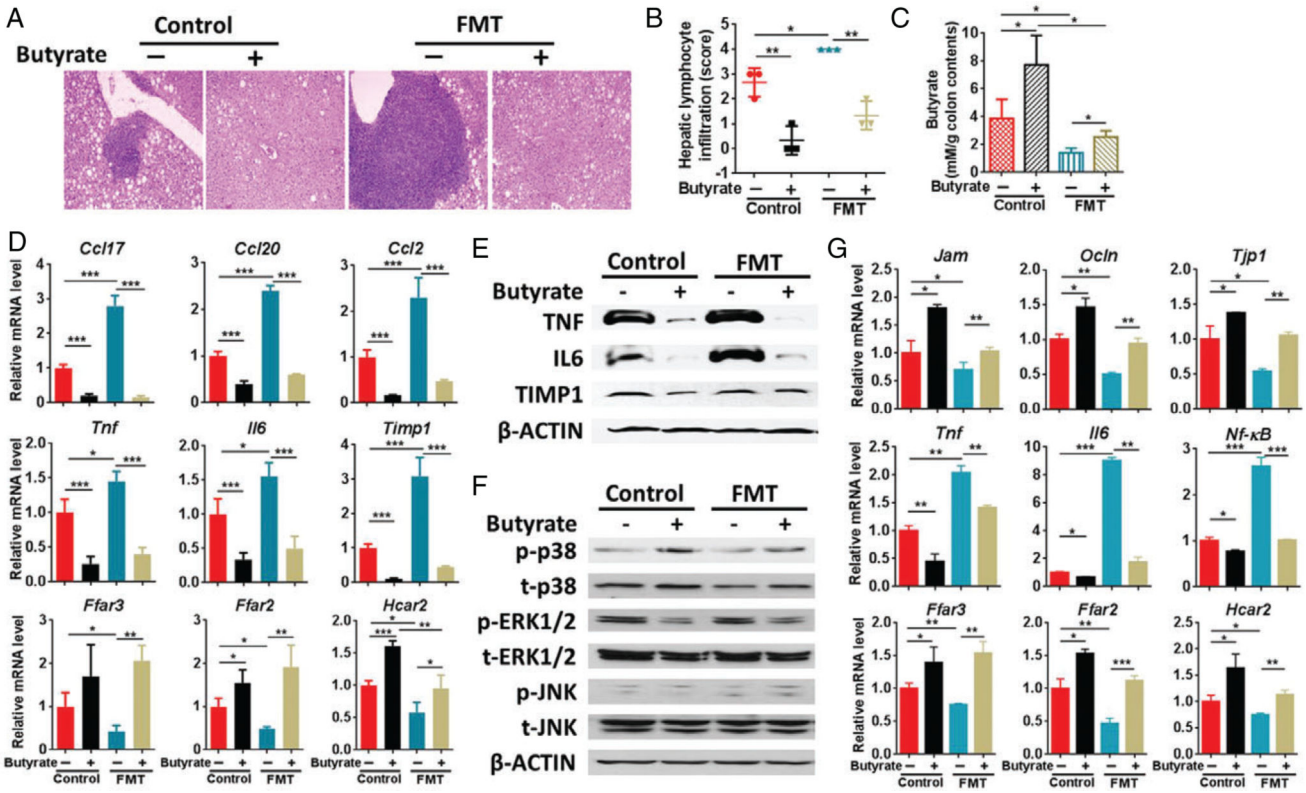

Figure 5.

Effect of butyrate in WD-fed FXR KO male mice with and without fecal microbiota transplantation (FMT). (A) Representative liver morphology and H&E-stained liver sections (original magnification 40×). (B) Hepatic lymphocyte infiltration score was graded on a scale of 0 (absent), 1 (rare), 2 (mild), 3 (moderate), and 4 (severe). (C) NMR analysis of butyrate concentration in colon contents. (D) Hepatic gene expression. (E) Western blot analysis of the indicated hepatic protein levels. (F) Western blot of MAPK pathways in the liver. (G) Colon gene expression. $n = 3$ per group. Data are expressed as mean ± SD. One-way ANOVA with Tukey's correction. *$p < 0.05$; **$p < 0.01$; ***$p < 0.001$.

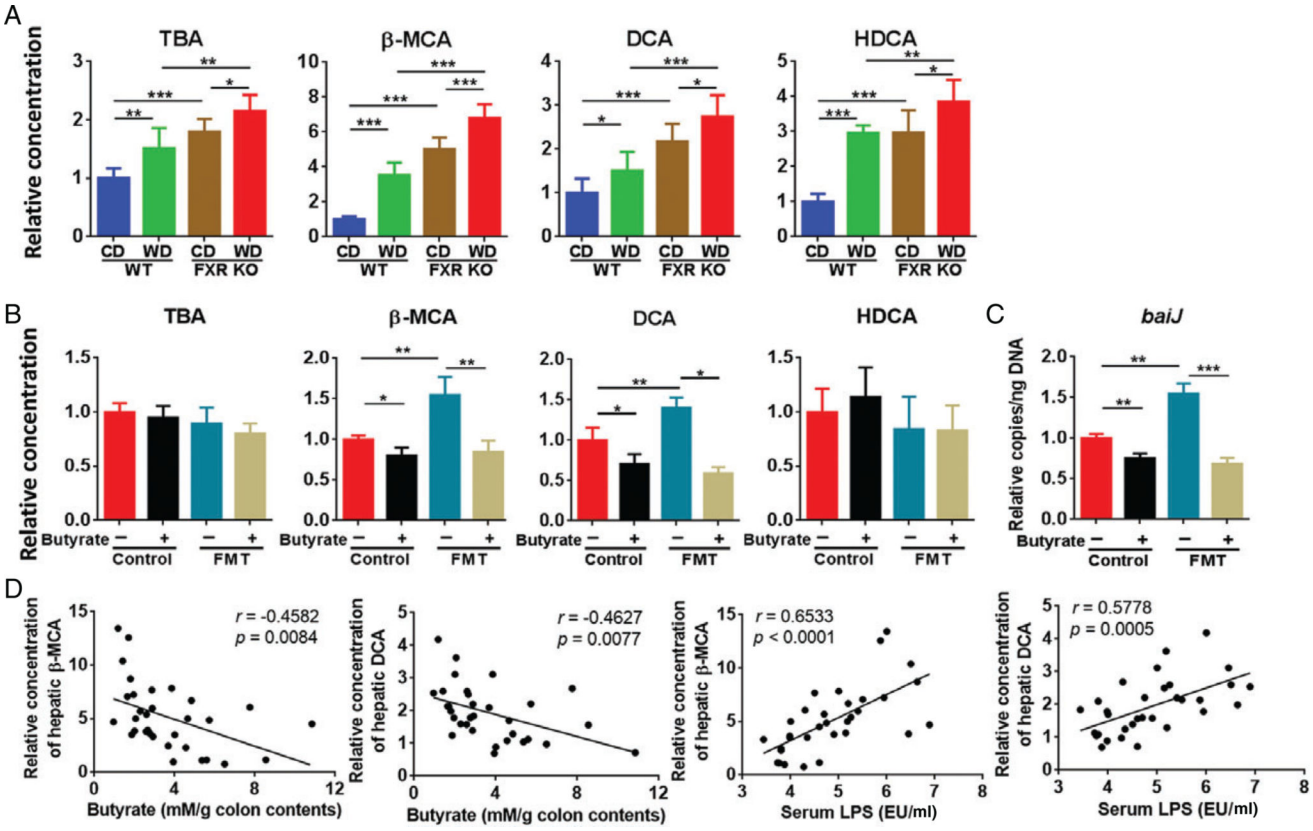

Figure 6.

Hepatic bile acid profile. (A) Relative concentration of hepatic total bile acid (TBA) and individual bile acids in CD- and WD-fed WT and FXR KO mice. $n = 8$ per group. (B) Relative concentration of hepatic TBA and individual bile acids in mice with and without fecal microbiota transplantation (FMT). $n = 3$ per group. (C) Relative copy number of fecal *baiJ*. $n = 3$ per group. (D) Correlation between the concentration of hepatic BAs and colonic butyrate as well as serum LPS level in all the studied mice. Each dot represents one mouse ($n = 32$). The straight line represents the best-fit line obtained by linear regression analysis. Data are expressed as mean ± SD. One-way ANOVA with Tukey's correction. *$p < 0.05$; **$p < 0.01$; ***$p < 0.001$.